A Dodecamethoxy [6]Cycloparaphenylene Consisting Entirely of Hydoroquinone Ether Units: Redox Properties and Host-Guest Complexation.

Naoki Narita,[a] Yusuke Kurita,[a] Kohtaro Osakada,[b] Tomohito Ide,*[c] Yoshitaka Tsuchido,*[a] and Hidetoshi Kawai*[a]

[a] Department of Chemistry, Faculty of Science, Tokyo University of Science, 1–3 Kagurazaka, Shinjuku-ku, Tokyo 162-8601, Japan
E-mail: tsuchido@rs.tus.ac.jp, kawaih@rs.tus.ac.jp
[b] Laboratory for Chemistry and Life Science, Institute of Innovative Research, Tokyo Institute of Technology, 4259, Nagatsuta, Midori-ku, Yokohama 226-8503, Japan
[c] Department of Chemical Science and Engineering, National Institute of Technology, Tokyo College, 1220-2 Kunugida-machi, Hachioji-shi, Tokyo, 193-0997, Japan
E-mail: ide@tokyo-ct.ac.jp

Dedicated to Professor Shigeru Yamago on the occasion of his 60th birthday

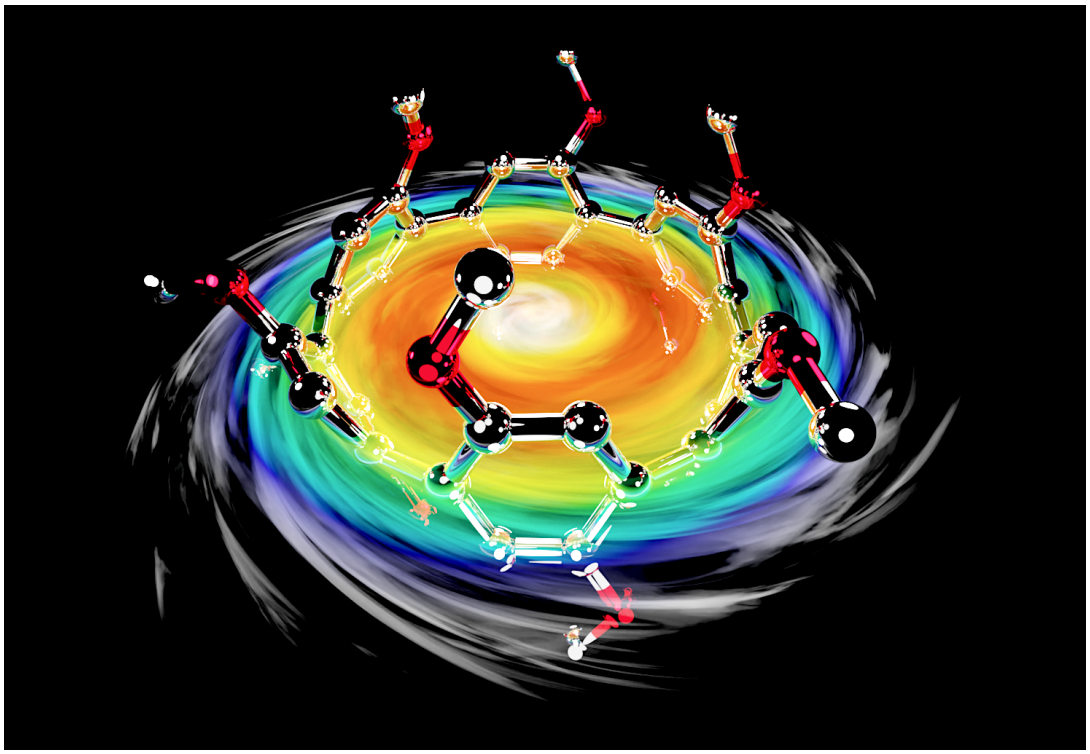

Abstract: *[6]Cycloparaphenylene derivative with twelve methoxy groups at the 2,5-positions of all benzene rings was synthesized via a macrocyclic gold complex. The compound adopts a cylindrical molecular structure with a planar chirality due to multiple introductions of methoxy groups, thereby including electron-deficient guest molecules, and is easily oxidized to give a dicationic compound that exhibits in-plane aromaticity.*

[*n*]Cycloparaphenylenes ([*n*]CPPs, where *n* is the number of phenylene groups), consisting of 1,4-linked phenylene unit, have attracted much attention due to their unique π-conjugated structures and physical properties.[1][2][3] Starting with the pioneering works in 2009-2010,[4][5][6] [*n*]CPPs with various ring sizes and functional groups have been successfully synthesized over the past decade. Accordingly, tuning of physical properties and functionalization applications such as supramolecular hosts by introducing functional groups to the aryl ring have also been studied.[7][8][9] In particular, the introduction of well-ordered functional groups on all aromatic rings of [*n*]CPPs can lead to the occurrence of a unique molecular topology and physical properties due to the macrocyclic molecular structure with a periodical array, such as Tanaka's alkoxy-bridged [*n*]CPPs (*n* = 8, 10) with belt or Möbius topologies,[10] Du's methoxy-functionalized [8]CPP,[11] and Itami's fully-fluorinated [*n*]CPPs (*n* = 10, 12, 14, 16) (Figure 1a).[12] On the other hand, there are no examples of functionalization of all benzene rings of [*n*]CPPs with a small ring size, especially smaller than [7]CPP, due to the strong ring strain and the steric hindrance of the substituents that hampers their synthesis, although partially halogenated [5] and [6]CPPs have been synthesized by Yamago (Figure 1b).[13][14]

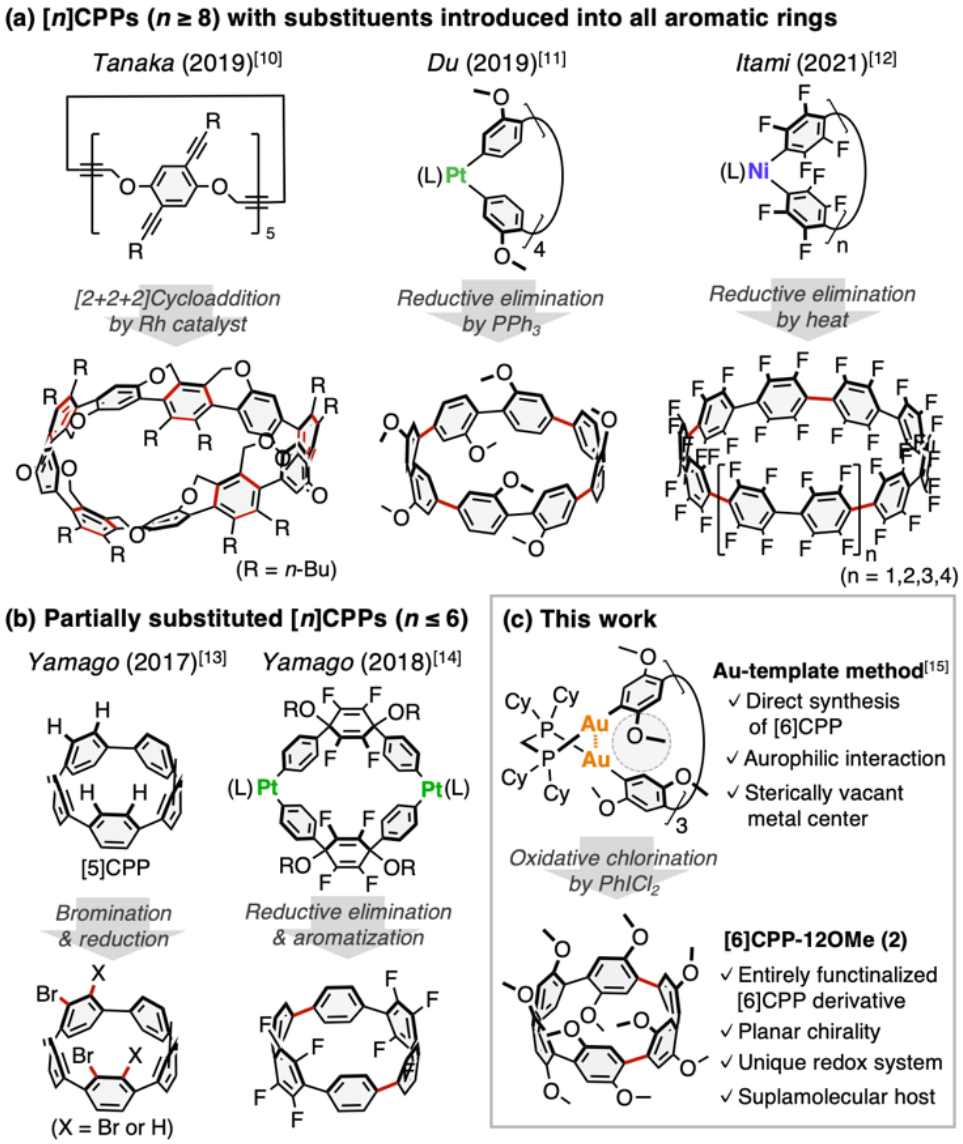

Figure 1. Synthesis of [*n*]cycloparaphenylene ([*n*]CPP) with multiple functional groups. (a) [*n*]CPPs ($n \geq 8$) with substituents introduced into all aromatic rings. (b) Partially substituted [*n*]CPPs ($n \leq 6$) with small ring size. (c) [6]Cycloparaphenylene derivatives with hydoroquinone ether units (2,5-dimethoxy groups) incorporated into all benzene rings from maclocyclic Au complex (This work).

Recently, we have developed a new synthetic method for the [*n*]CPPs (n = 6, 9-15) *via* a macrocyclic gold complex.[15][16] A notable feature of this method is that it employs a triangular-shaped macrocyclic gold complex with Au_2-diphosphine units located at the three corners that have stabilized their molecular structure through the

aurophilic interactions[17][18][19][20]. We considered that our synthetic method would be suitable for the multi-functionalization of [*n*]CPPs with small ring size for the following reasons; i) the aurophilic interactions have degrees of freedom in their bond distances and angles, allowing the formation of the macrocyclic structure even when the multi-functionalization leads to crowding around the Au complex, ii) a Au(I) center coordinates only one aryl ligand, providing a more sterically vacant metal center than the biaryl M(II) complexes (M = Ni, Pd, Pt), and there would be less steric repulsion between the aryl ligands even if the substituents are introduced at the *ortho*-position (Figure 1c).

In this study, we report the synthesis of the [6]cycloparaphenylene derivative with hydoroquinone ether units (2,5-dimethoxy groups) incorporated into all benzene rings by employing the Au-templated CPP synthesis method, and their electrochemical properties and host-guest chemistry. Gaeta *et al.* reported the synthesis of a [8]CPP derivative incorporating one 2,5-dimethoxyphenylene ring and the inclusion ability toward methylpyridinium salts (K_a = 2.2 × 10^3 M^{-1}, $CDCl_3$, 25 °C)[21]. Du *et al.* reported the synthesis of a [8]CPP derivative with several 2,5-dimethoxy groups,[22] and that the molecule did not show significant inclusion ability toward various electron-deficient guest molecules. The averaged diameter of [6]CPP is 8.07 Å,[23][24] which is comparable to that of pillar[5]arenes (ca. 9.0 Å),[25] and is expected to recognize guest molecules with a size of alkyl chains that have not been achieved for the CPP system.

The reaction of 2,2',5,5'-tetramethoxy-1,1'-biphenyl-4,4'-diyl diboronic acid (**L2**) with $[Au_2Cl_2(dcpm)]$ (dcpm = bis(dicyclohexylphosphino)methane) in the presence of Cs_2CO_3 (1.0:1.0:6.0 molar ratio) in toluene/ethanol/water at 50 °C produced the macrocyclic Au complex, $[Au_2(C_6H_4\text{-}2,5\text{-}(OMe)_2)_2(dcpm)]_3$ (**Au-2**), in 83% isolated yield. Then, the oxidative chlorination[26] of **Au-2** occurs upon the addition of $PhICl_2$ in

CH_2Cl_2 at 25 °C for 4 h. The reaction mixture was purified by silica gel column chromatography to give [6]CPP-12OMe (**2**) in 52% yield over 2 steps (Figure 2a).

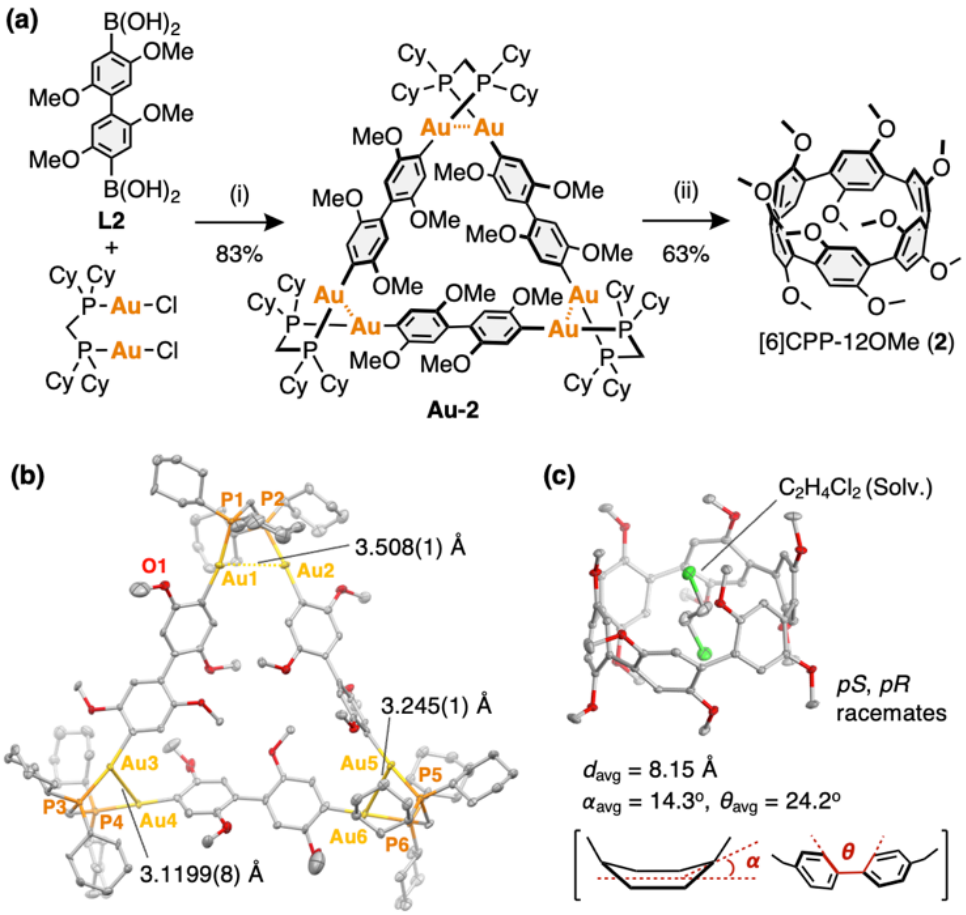

Figure 2. Synthesis and characterization of [6]CPP-12OMe (**2**): (a) synthetic route for **2**. reagents and conditions; (i) Cs_2CO_3 (6.0 equiv.), toluene/EtOH/H_2O, 50 °C, 20 h, (ii) $PhICl_2$ (3.0 equiv.), DMF, -60 °C to r.t., 3 h. ORTEP drawing of (b) **Au-2** and (c) **2** (30% level of probability). Hydrogen atoms are omitted for clarity.

The molecular structure of macrocyclic Au complex (**Au-2**) was confirmed by X-ray crystallography (Figure 2b). The complex adopted the triangular shaped structure with twisted Au-P-C-P-Au groups at the three corners, similar to that the non-substituted Au complex, $[Au_2(C_6H_4)_2(dcpm)]_3$, reported in our previous study.[15] The distance

between the two neighboring gold atoms in helical corners (3.508(1), 3.245(1), 3.1199(8) Å) are observed to be as significantly longer than that of $[Au_2(C_6H_4)_2(dcpm)]_3$ (3.1799(11) 3.0696(8) Å) (see supporting Figure S27), which indicates that the triangular structure can be maintained even when the bulky methoxy groups are introduced at the *ortho* positions of the arylene linkers. This result clearly showed that our Au-templated method has a wide range of substrate applicability.

The single crystals of **2** suitable for X-ray crystallography were obtained *via* the vapor diffusion of *n*-hexane into 1,2-dichloroethane solution of the molecule. The crystal structure was analyzed as 1,2-dichloroethane incorporated structure (Figure 2c). The all-methoxy groups of the dimethoxybenzenes are oriented in the same direction in the molecule, resulting in two stereo isomers, *pR* and *pS*, with planar chirality depending on the orientation of the methoxy groups. The molecule adopted an elliptical molecular structure similar to [6]CPP with a slightly lengthened diameter (avg. 8.15 Å). Interestingly, the averaged dihedral angle between two phenylene rings (θ_{avg}) was estimated to be 24.2°, which is narrower than that of [6]CPP (28.1°).[23][24] Rathore reported synthesis, molecular structure, and electrochemical properties of oligo(*p*-phenylene)s with 2,5-dimethoxy groups, $(C_6H_4\text{-}2,5\text{-}OMe)_nH_2$ (n = 2-9)[27], which are a linear analog of **2.** The dihedral angle (56°) in the crystal structure of $(C_6H_4\text{-}2,5\text{-}OMe)_3H_2$ was significantly wider than that of *p*-terphenyl (≤ 1°)[28], which is in contrast to that of the CPP system in this study. The small dihedral angle of **2** would be due to its macrocyclic structure, which restricts the change of dihedral angle, resulting in a tubular molecular conformation that can minimize steric repulsion with the methoxy groups.

The above-mentioned molecular conformations in the crystal structures have also been in solution. The ^{1}H NMR signal of arylene protons of **2** appeared as a slightly

broad singlet peak at 7.34 ppm (400 MHz, $CDCl_3$, 298 K). The fact that the corresponding signal of $(C_6H_4\text{-}2,5\text{-}OMe)_nH_2$[27] was observed in 6.9 ppm suggests that all arylene rings of **2** are oriented perpendicular to the CPP macroring as in the crystal structure, and thus the downfield shift of the Ar-H proton of **2** compared to that of $(C_6H_4\text{-}2,5\text{-}OMe)_nH_2$ would be attributed to less shielding effects from the other arylene rings due to the small Ar-Ar dihedral angles. The variable-temperature NMR measurements, DFT calculations, and chiral HPLC analysis suggested that the ring flipping of **2** occurred rapidly, and that the two stereoisomers are fast exchanging in solution (see supporting Figure S10-12).

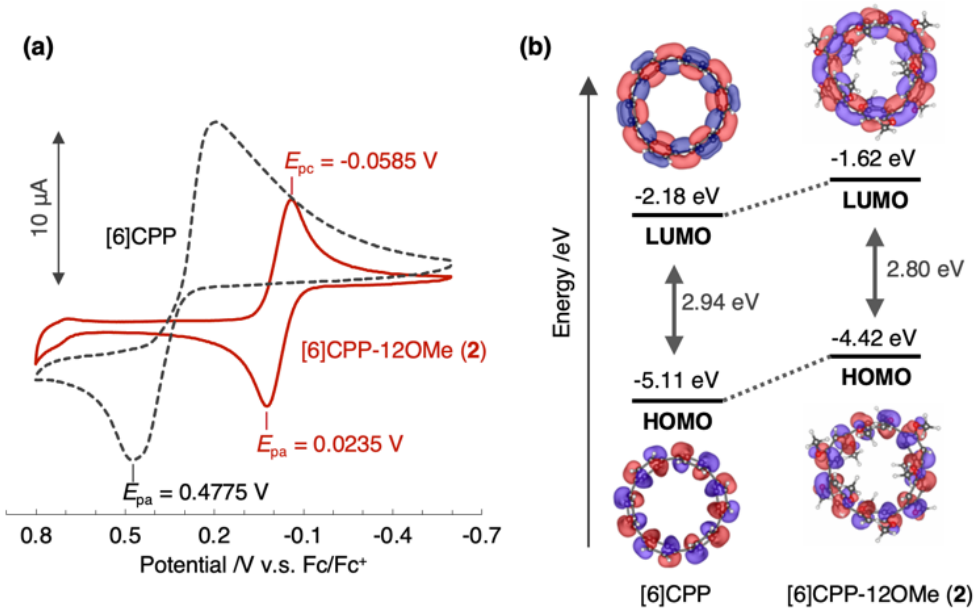

Figure 3. (a) Cyclic voltammograms of [6]CPP-12OMe (**2**) (red line) and [6]CPP (dotted line) (CH_2Cl_2, [M] = 1.0 x 10^{-3} M, electrolyte: 0.1 M $TBAPF_6$, scan rate: 100 mV s^{-1}, r.t.) (b) Energy diagrams and Kohn-Sham orbitals of [6]CPP-12OMe (**2**) (right) and [6]CPP (left) (B3LYP/def2-SVP//TPSS-D3(BJ)/def2-SVP, isosurface; 0.02).

The cyclic voltammogram of **2** showed the reversible redox wave with $E_{1/2}$ = 0.0041 V vs. Fc/Fc^+ (E_{pa} = 0.0235 V, E_{pc} = -0.0585 V), which is drastically lower potential

than that of [6]CPP (E_{pa} = 0.4775 V)[23][24] (Figure 3a). To understanding the difference in the electrochemical properties, the frontier orbitals were simulated by DFT calculations using ORCA[29] (Figure 3b). Interestingly, although the shape of the frontier orbitals was comparable, the HOMO and LUMO levels of **2** (-4.42, -1.62 eV) were found to be drastically higher than those of [6]CPP (-5.11, -2.18 eV). The significant increase in these levels would be due to i) the effect of the electron-donating nature of the methoxy groups and ii) the increase in ring strain and π-conjugation based on the decrease in Ar-Ar dihedral angle caused by the steric hindrance of the methoxy groups.[30]

The chemical oxidation of **2** with $[N(C_6H_4\text{-}4\text{-}Br)_3]SbCl_6$ (*Magic Blue*, ***MB***) was monitored by UV-Vis-NIR spectra (Figure 4a). In the neutral state, [6]CPP-12OMe (**2**) showed absorptions at 320 and 390 nm in the UV region and a broad absorption around 450-600 nm, resulting in a reddish-brown color. Upon additions of 0.5 and 1.0 eq. of ***MB***, a broad absorption over the near-infrared region was observed (λ_{max} = 1400 nm), turning a green solution. Further addition of ***MB*** up to 2.0 eq. increased the absorption around 1400 nm and absorptions at 615 and 970 nm appeared, and the solution turned blue. These results are similar to those reported by Yamago[31][32][33][34] about the formation of cation radicals (**[6]CPP**$^{\bullet+}$) (λ_{max} = 1136 nm) and dication (**[6]CPP**$^{2+}$) (λ_{max} = 464, 792 nm) in the multi-step oxidation of [6]CPP by $(NO)SbCl_6$ (Figure 4b). The TD-DFT calculations suggested the formation of radical cation (**2**$^{\bullet+}$) (λ_{DFT} = 1334 nm) and dication (**2**$^{2+}$) (λ_{DFT} = 971 nm), respectively. The electron density difference of the first excited states in both **2**$^{\bullet+}$ and **2**$^{2+}$ suggests an electron donation from the methoxy groups regarding the red shifts of the absorption bands (See supporting information, Table S4-6).

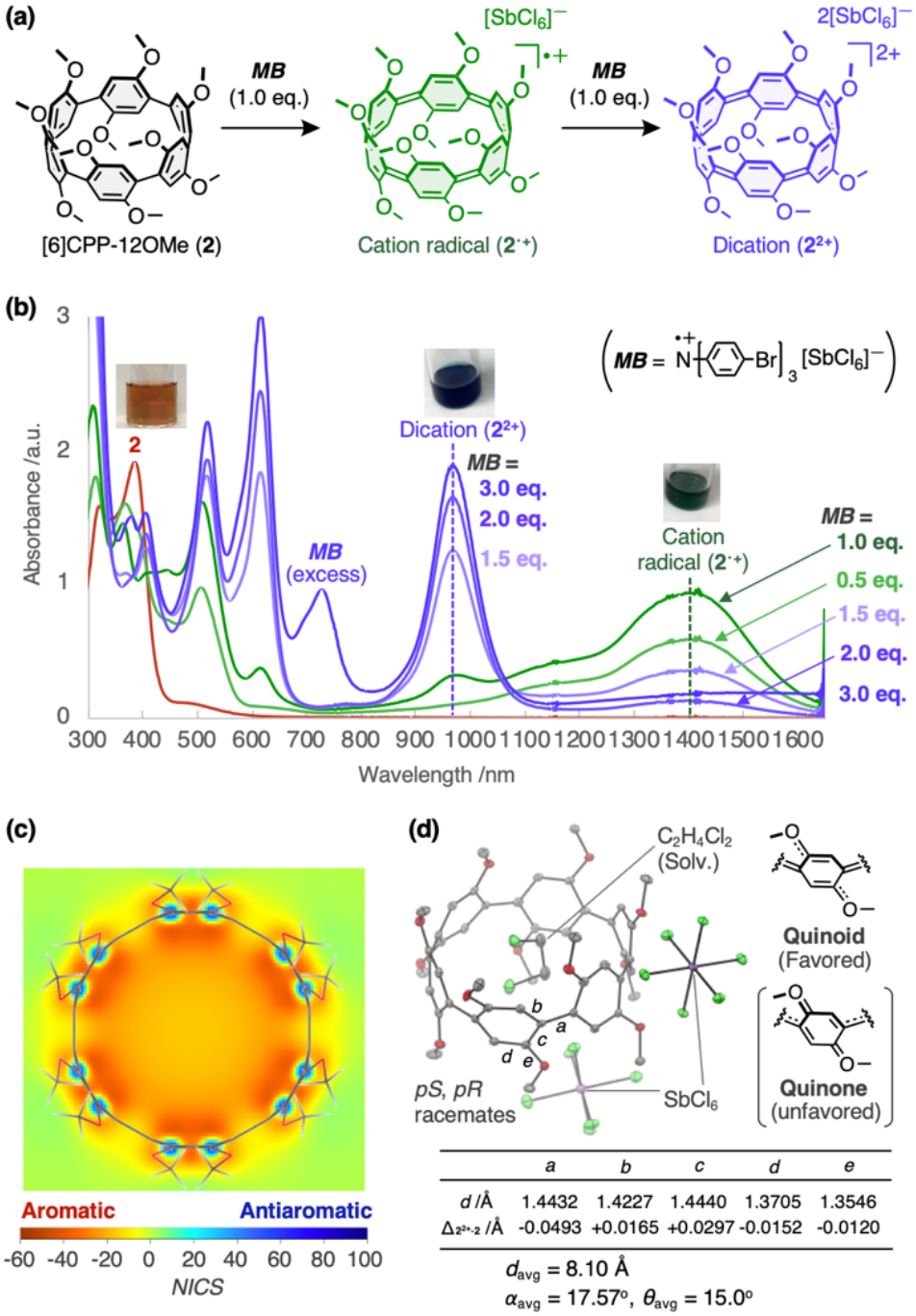

Figure 4. (a) Chemical oxidation of [6]CPP-12OMe (**2**) with $[N(C_6H_4\text{-}4\text{-}Br)_3]SbCl_6$ (*Magic Blue*, ***MB***). (b) UV-vis-NIR titration of **2** with ***MB*** (CH_2Cl_2, [**2**] = 1.5 x 10^{-5} M, r.t.) (c) 2D-NICS (nucleus-independent chemical shifts) plot of dication ($\mathbf{2}^{2+}$). (d) ORTEP drawing of $\mathbf{2}^{2+}$ (30% level of probability). Hydrogen atoms are omitted for clarity.

The formation of dication ($\mathbf{2}^{2+}$) was also confirmed by ^{1}H NMR spectroscopy. The chemical shift of the aryl protons was shifted from 7.34 ppm to 5.74 ppm by addition of 2 eq. of ***MB*** ($CDCl_3$, 298 K, See supporting information, Figure S14), which is due to the shielding effect caused by a generation of an in-plane aromaticity. [32] The results of the nucleus-independent chemical shifts (NICS) calculation also support the in-plane aromaticity of the oxidized species (Figure 4c).

A single crystal of the $\mathbf{2}^{2+}$ was obtained by vapor diffusion (1,2-dichloroethane/*n*-hexane), and the structure was successfully analyzed by X-ray crystallography (Figure 4d). This is the smallest ring-size CPP dication that has been successfully determined by X-ray crystallography, although Yamago reported the crystal structure of [8]CPP dication.[31] The harmonic oscillator model of aromaticity (HOMA) value of each 6-membered ring in $\mathbf{2}^{2+}$ was calculated to be 0.585, which was a significant decrease of more than 0.3 over those of the neutral species **2** (0.895), indicating that the benzene rings in the dication adopt a quinoid-like structure resulting in the loss of aromaticity of the benzene ring. The bond alternation analysis of **2** and $\mathbf{2}^{2+}$ revealed that the arylene units of $\mathbf{2}^{2+}$ prefers a quinoid-like structure rather than quinone-like structure. According to the study on the oxidation of $(C_6H_4\text{-}2,5\text{-}OMe)_nH_2$ (n = 2-9) by Rathore,[27] the linear oligomers favored the quinone-like structure with the large dihedral angle, and the positive charge being localized to a part of the arylene ring(s), which are in contrast with the results of $\mathbf{2}^{2+}$.

[6]CPP-12OMe (**2**) adopts the cylindrical molecular structure with extremely electron-rich aryl rings owing to the multi-substituted methoxy groups, promising applications in host-guest chemistry. First, to investigate the scope of guest applicability for **2**, we have mixed **2** and various guest molecules in $CDCl_3$ and found that the chemical

shift of the Ar-H protons changed significantly toward *n*-alkanes with an electron-deficient group such as cyano, *N*-pyridinium, azide, and isocyanate groups. On the other hands, mixing with guest molecules with branched chain (e.g. cyanoalkane with branched chain, and trialkylammonium salt) and with electron-rich molecules (e.g., PEG) did not affect the chemical shift of the Ar-H protons (see supporting Figure S18-21).

The complexation of **2** with NC-$(CH_2)_4$-CN (adiponitrile, **G1**) was confirmed by ^{1}H NMR titrations (Figure 5a). The addition of **G1** upon a $CDCl_3$ solution of **2** (0.5 mmol L^{-1}, 298 K) caused a downfield shift of the ^{1}H NMR signals of aryl and methoxy protons (Figure 5b), indicating the formation of a supramolecular complex with a faster equilibrium rate than the ^{1}H NMR timescale. The association constant (K_a) was estimated to be 186 M^{-1} ($CDCl_3$, 298 K).[35] The change in chemical shift would be caused by deshielding of protons due to a decrease in the dihedral angles (θ) accompanying a guest inclusion, rather than by an electrostatic interaction between the host and guest molecules. Use of symmetry adaptive perturbation theory (SAPT) calculations[36] with PSI4[37] to decompose the interaction energies for different conformations and positions of **G1** in the inclusion complex (**2⊃G1**) showed that having **G1** located inside the cavity with the *gauche*-conformation brings the CH_2 unit closer to the aylene unit, which affects the electrostatic and dispersion forces more effectively than the *anti*-conformation (Figure 5c). In addition, the *gauche*-conformation also enables a stronger electrostatic interaction between the terminal cyano group and electron-rich skeleton of **2** because of closer to each other than the *anti*-conformation. The closer guest-host contact enforces the dispersion force, which is in turn offset (to some extent) by the increased exchange repulsion.

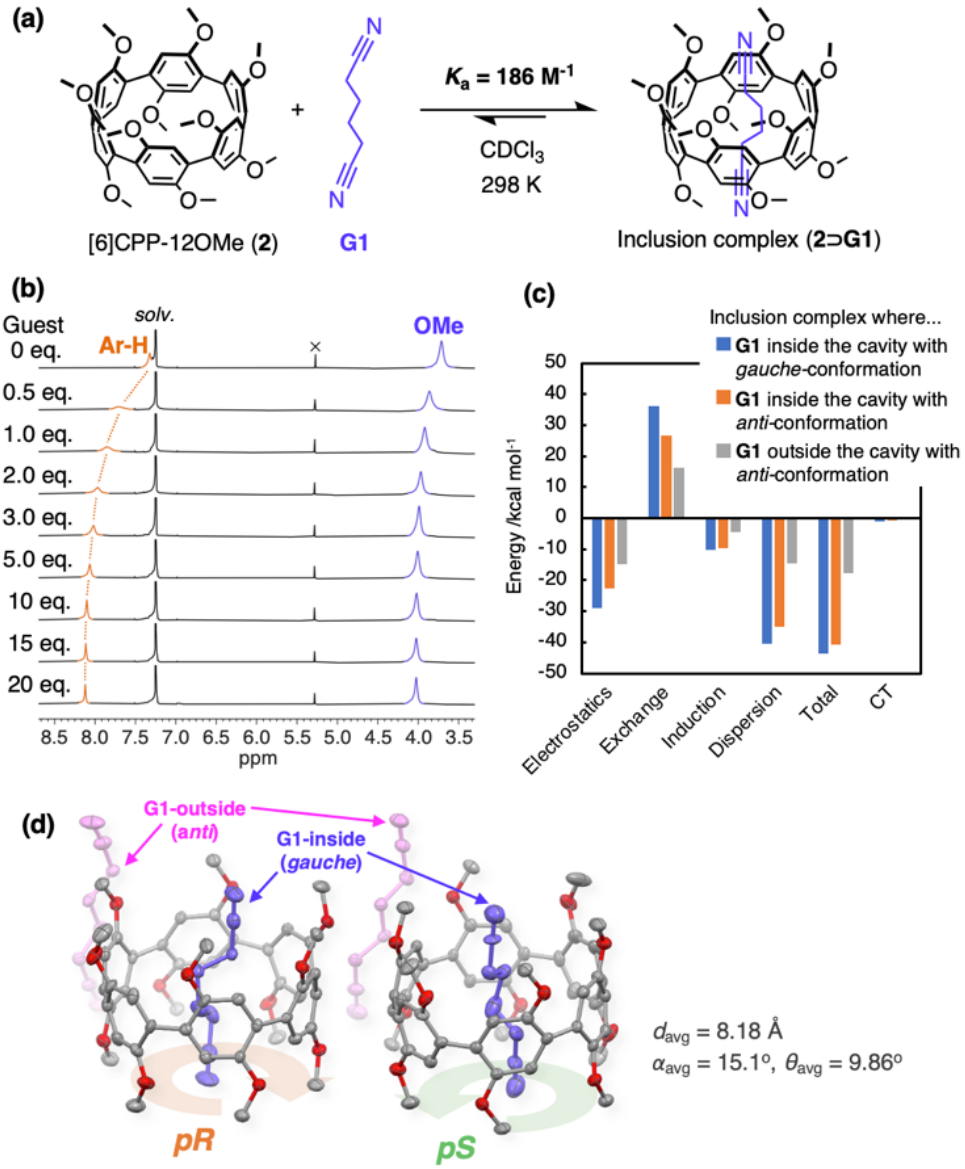

Figure 5. (a) Formation of inclusion complex (**2⊃G1**) between [6]CPP-12OMe (**2**) and NC-$(CH_2)_4$-CN (adiponitrile, **G1**). (b) ^{1}H NMR titration of **2** with **G1** (400 MHz, $CDCl_3$, r.t.). (c) Interaction energy decomposition by symmetry-adapted perturbation theory (SAPT) calculation of inclusion complex (**2⊃G1**) with different positions and orientations of **G1** relative to **2** (SAPT0/jul-cc-pVDZ level of theory). (d) ORTEP drawing of inclusion complex (**2⊃G1**) (30% level of probability). Hydrogen atoms are omitted for clarity.

A single crystal of the inclusion complex (**2⊃G1**) suitable for single crystal X-ray crystallography was obtained by slow diffusion of *n*-hexane vapor into a $CHCl_3$

solution of **2** with an excess amount of **G1** (Figure 5d). The two stereoisomers of **2** (*pR* and *pS*) and four **G1** molecules are in an asymmetric unit cell ($P2_1/c$). Two **G1** molecules are located inside of the cavity of two **2** molecules with a *gauche*-conformation, whereas another two **G1** molecules are located outside of the macrocycle with an *anti*-conformation. The averaged dihedral angle (θ_{avg}) of inclusion complex (**2⊃G1**) was estimated to be 9.86°, which is drastically reduced from that of 1,2-dichloroethane incorporated structure (24.2°) shown in Figure 2c. The guest molecule inside the cavity of **2** adopts an entropically unfavorable the *gauche*-conformation, and multiple intermolecular CH-π interactions were formed between the alkyl hydrogens of **G1** and the aryl rings of **2**. These results suggest that the inclusion of **G1** is enthalpy-driven process caused by the combination of dispersion and electrostatic interactions between host and guest molecules, which has been supported by the results of the SAPT calculations (Figure 5c). This is a first example of CPP encapsulating a guest molecule with a flexible alkyl structure, which is achieved by the electron-rich aryl rings with the methoxy groups.

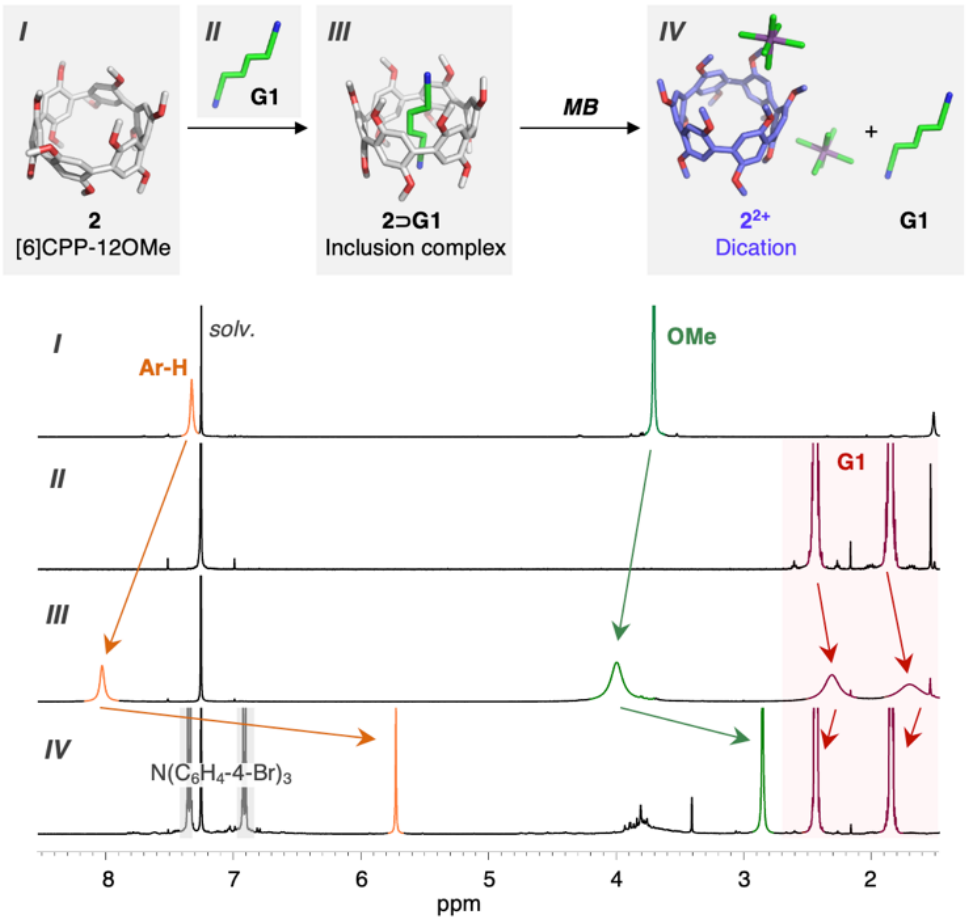

Figure 6. ^{1}H NMR monitoring for On-Off switching in the formation/deformation of inclusion complex (**2⊃G1**) by chemical oxidation (400 MHz, $CDCl_3$, r.t.). (I) [6]CPP-12OMe (**2**), (II) adiponitrile (**G1**), (III) inclusion complex (**2⊃G1**) ([**2**] = 5.0 μmol L^{-1}, [**G1**] = 22.6 μmol L^{-1}), (IV) addition of 2 eq. of ***MB*** (10 μmol L^{-1}) to **2⊃G1.**

Interestingly, the dication ($\mathbf{2}^{2+}$) did not recognize any of guest molecules (see supporting Figure S25), including those bound in the neutral state, probably because the benzene rings became a quinoid structure and could not form CH-π interactions to the guest molecules effectively. By utilizing the oxidation reaction of **2** and the resulting change in the guest inclusion capacity, we achieved the On-Off switching in the formation/deformation of the inclusion complex of **2** with **G1** (Figure 6). Upon addition of **G1** to a $CDCl_3$ solution of **2**, the proton signals of **2** shifted to the downfield, while the

signals of **G1** broadened and shifted to the upfield (Figure 6, III), accompanying the formation of the inclusion complex. By adding the oxidant (***MB***) to the solution, a upfield shift of the aryl proton of **2** to 5.74 ppm was observed, while the signal of **G1** returned to the original position (Figure 6, IV). These results indicate that the **G1** dissociated from **2** by the formation of $\mathbf{2}^{2+}$.[38]

Finally, we applied the function of [6]CPP-12OMe (**2**) as a supramolecular host to the synthesis of a mechanically interlocked molecule (MIM)[39] with a planar chirality. Mixing **2** with an excess amount of OCN-$(CH_2)_6$-NCO (hexamethylene diisocyanate) in $CHCl_3$ to form a pseudo[2]rotaxane *in situ*, then introducing a bulky substituent at the both ends of the axle molecule through a urea bond formation reaction with 1-adamantanemethylamine produced a [2]rotaxane (**1**) containing **2** as a ring component (Figure 7a). The chiral HPLC analysis of **1** observed two peaks with the retention times of 12.5 and 13.2 min, respectively (see supporting Figure S10b). This result indicates that the interpenetration of the alkyl chain to the cavity of **2** prevented the p*R* ⇔ p*S* racemization through a sequence of "oxygen-through-the-annulus" inside-out and outside-in rotations as seen in pillar[*n*]arene[40].

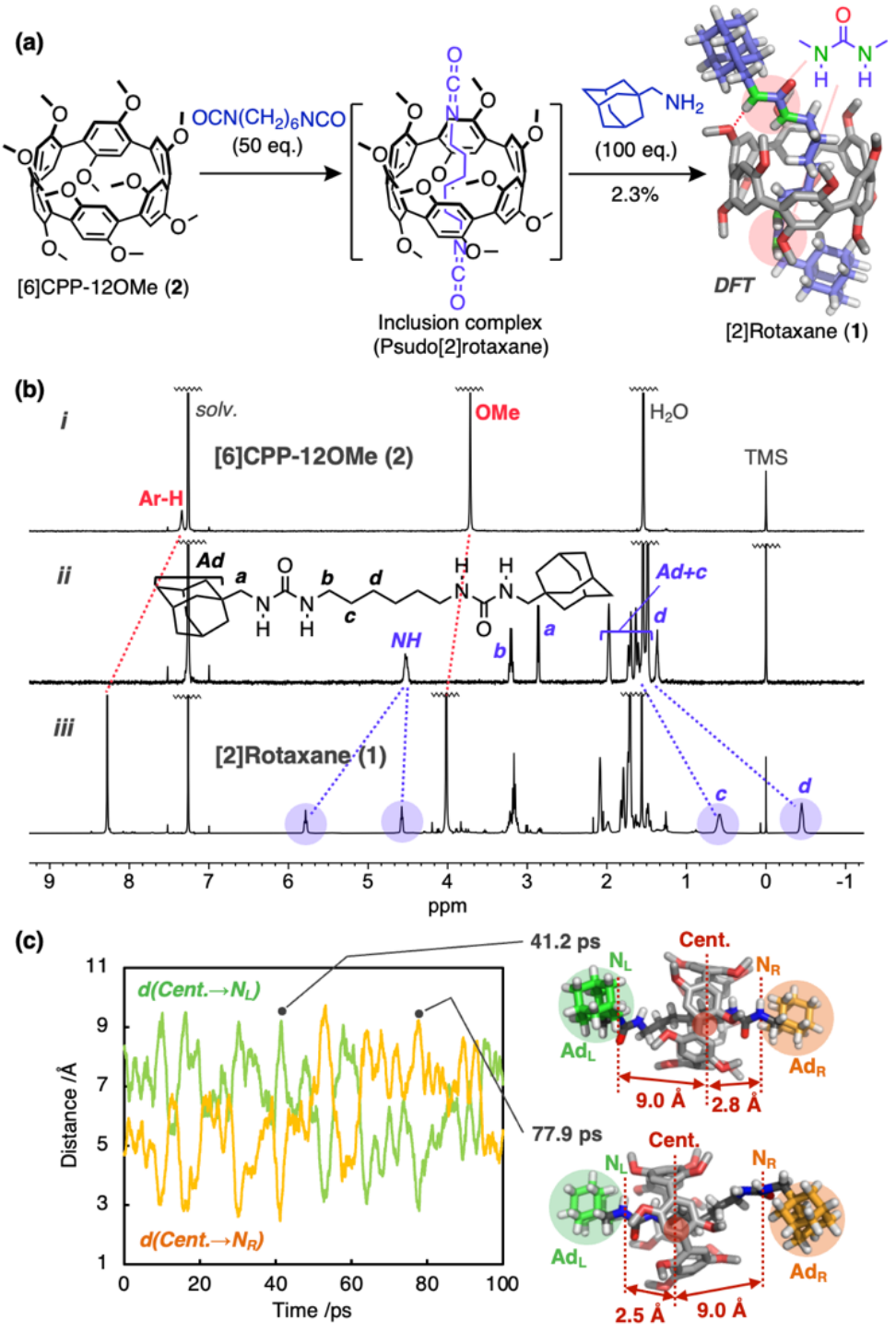

Figure 7. Synthesis and characterization of [2]rotaxane (**1**): (a) synthetic route for **1**. Molecular model of **1** was optimized by DFT calculations. Hydrogen atoms of CPP unit were omitted for clarity. (b) Stacked ^{1}H NMR spectra of (i) [6]CPP-12OMe (**2**), (ii) axle molecule, $(C_{10}H_{15})CH_2NHCONH(CH_2)_6NHCONHCH_2(C_{10}H_{15})$, and (iii) [2]rotaxane (**1**) (400 MHz, $CDCl_3$, r.t.).

(c) Time variation of distance change between the centroid of CPP macroring and outer nitrogen atom in the axle calculated by molecular dynamics (MD) simulations.

In the ^{1}H NMR spectrum of racemate of **1** (Figure 7b, iii), the chemical shifts of the CH_2 protons of the axle component (H_c, H_d) were observed around 0.9 to -0.5 ppm, which are upfield region than that of free axle molecule (Figure 7b, ii). These shifts are attributed to the shielding effect from the arylene rings of **2**, indicating that the alkyl chain is mechanically interlocked inside the cavity of **2**. On the other hands, one of the NH protons of the urea groups shifted significantly to a downfield position at 5.79 ppm, which is due to the formation of NH…O hydrogen bonds between NH proton and methoxy oxygens of **2**. The formation of NH…O hydrogen bonds was also observed in the stable conformation of **1** as estimated by DFT calculations (Figure 7a). These results suggest that the terminal urea groups function as a ‘‘station’’, and that the CPP macrocycle undergoes a rapid shuttling movement along the alkyl chain of the axle component, which is also supported by the molecular dynamics (MD) calculations (Figure 7c).

Delius *et al.* reported the synthesis of [2]rotaxane with [10]CPP as the ring component and fullerene (C_{60}) as the axle and the endcap groups.[41] In that case, the CPP macrocycle rotates around C_{60} moiety because of the strong interaction between [10]CPP and C_{60}. Thus, we succeeded in developing a new CPP-based molecular machine that imparts a higher order of mechanical motion by utilizing the interaction between methoxy groups introduced into [6]CPP and the urea moieties of the axle component. This molecule offers the potential for new supramolecular system utilizing their planar chiral mechanically interlocked structure, redox ability of CPP unit, and an anion-binding property of urea moieties.[42]

In this study, we have succeeded in synthesizing [6]cycloparaphenylene with twelve methoxy groups, [6]CPP-12OMe (**2**), by our developed synthetic method *via* macrocyclic gold complex. This result clearly demonstrates that our method could be useful for the synthesis of [*n*]CPPs with a small ring size and multiply substituted arene rings. [6]CPP-12OMe (**2**) has an extremely high HOMO level compared to the unsubstituted [6]CPP caused by the electron-donating ability of the methoxy groups and the smaller Ar-Ar dihedral angles, allowing facile oxidation to give dicationic species with in-plane aromaticity. Furthermore, [6]CPP-12OMe (**2**) functions as a supramolecular host molecule with a fully π-conjugated framework, and successfully included guest molecules with a flexible alkyl chain which can be controlled by the chemical oxidation. By applying the ability of [6]CPP-12OMe (**2**) to function as a supramolecular host, we succeeded in creating the CPP-based molecular machine.

Acknowledgements

This work was financially supported by JSPS KAKENHI grant numbers JP19K15533 (Grant-in-Aid for Young Scientists), 21K05093 (Grants-in-Aid for Scientific Research (C)), and 21H05496 (Grants-in-Aid for Transformative Research Area (A), *Condensed Conjugation*).

Conflict of interest

The authors declare no conflict of interest.

Keywords: Cycloparaphenylenes • Au(I) Complex • Host-Guest Chemistry • In-plane Aromaticity • Rotaxane

References

[1] S. Yamago, E. Kayahara, T. Iwamoto, *Chem. Rec.* **2014**, *14*, 84–100.

[2] E. R. Darzi, R. Jasti, *Chem. Soc. Rev.* **2015**, *44*, 6401–6410.

[3] Y. Segawa, A. Yagi, K. Matsui, K. Itami, *Angew. Chemie - Int. Ed.* **2016**, *55*, 5136–5158.

[4] R. Jasti, J. Bhattacharjee, J. B. Neaton, C. R. Bertozzi, *J. Am. Chem. Soc.* **2008**, *130*, 17646–17647.

[5] H. Takaba, H. Omachi, Y. Yamamoto, J. Bouffard, K. Itami, *Angew. Chemie - Int. Ed.* **2009**, *48*, 6112–6116.

[6] S. Yamago, Y. Watanabe, T. Iwamoto, *Angew. Chemie - Int. Ed.* **2010**, *49*, 757–759.

[7] Y. Xu, M. von Delius, *Angew. Chemie - Int. Ed.* **2020**, *59*, 559–573.

[8] M. Hermann, D. Wassy, B. Esser, *Angew. Chemie - Int. Ed.* **2020**, 2–26.

[9] D. Lu, Q. Huang, S. Wang, J. Wang, P. Huang, P. Du, *Front. Chem.* **2019**, *7*, 1–9.

[10] S. Nishigaki, Y. Shibata, A. Nakajima, H. Okajima, Y. Masumoto, T. Osawa, A. Muranaka, H. Sugiyama, A. Horikawa, H. Uekusa, H. Koshino, M. Uchiyama, A. Sakamoto, K. Tanaka, *J. Am. Chem. Soc.* **2019**, *141*, 14955–14960.

[11] S. Cui, G. Zhuang, J. Wang, Q. Huang, S. Wang, P. Du, *Org. Chem. Front.* **2019**, *6*, 1885–1890.

[12] H. Shudo, M. Kuwayama, M. Shimasaki, T. Nishihara, Y. Takeda, N. Mitoma, T. Kuwabara, A. Yagi, Y. Segawa, K. Itami, *Nat. Commun.* **2022**, *13*, 3713.

[13] E. Kayahara, R. Qu, S. Yamago, *Angew. Chemie - Int. Ed.* **2017**, *56*, 10428–10432.

[14] S. Hashimoto, E. Kayahara, Y. Mizuhata, N. Tokitoh, K. Takeuchi, F. Ozawa, S. Yamago, *Org. Lett.* **2018**, *20*, 5973–5976.

[15] Y. Tsuchido, R. Abe, T. Ide, K. Osakada, *Angew. Chemie - Int. Ed.* **2020**, 22928–22932.

[16] Y. Yoshigoe, Y. Tanji, Y. Hata, K. Osakada, S. Saito, E. Kayahara, S. Yamago, Y. Tsuchido, H. Kawai, *JACS Au* **2022**, *2*, 1857–1868.

[17] H. Schmidbaur, *Chem. Soc. Rev.* **1995**, 391–400.

[18] H. Schmidbaur, *Gold Bull.* **2000**, *33*, 3–10.

[19] H. Schmidbaur, A. Schier, *Chem. Soc. Rev.* **2008**, *37*, 1931–1951.

[20] H. Schmidbaur, A. Schier, *Chem. Soc. Rev.* **2012**, *41*, 370–412.

[21] P. Della Sala, C. Talotta, T. Caruso, M. De Rosa, A. Soriente, P. Neri, C. Gaeta, *J. Org. Chem.* **2017**, *82*, 9885–9889.

[22] D. Lu, G. Zhuang, H. Jia, J. Wang, Q. Huang, S. Cui, P. Du, *Org. Chem. Front.* **2018**, *5*, 1446–1451.

[23] J. Xia, R. Jasti, *Angew. Chemie - Int. Ed.* **2012**, *51*, 2474–2476.

[24] E. Kayahara, T. Iwamoto, T. Suzuki, S. Yamago, *Chem. Lett.* **2013**, *42*, 621–623.

[25] T. Ogoshi, S. Kanai, S. Fujinami, T. Yamagishi, *J. Am. Chem. Soc.* **2008**, *130*, 5022–5023.

[26] W. J. Wolf, M. S. Winston, F. D. Toste, *Nat. Chem.* **2014**, *6*, 159–164.

[27] M. V. Ivanov, V. J. Chebny, M. R. Talipov, R. Rathore, *J. Am. Chem. Soc.* **2017**, *139*, 4334–4337.

[28] J. L. Baudour, H. Cailleau, W. B. Yelon, *Acta Crystallogr. Sect. B Struct. Crystallogr. Cryst. Chem.* **1977**, *33*, 1773–1780.

[29] F. Neese, *Wiley Interdiscip. Rev. Comput. Mol. Sci.* **2012**, *2*, 73–78.

[30] Y. Segawa, A. Fukazawa, S. Matsuura, H. Omachi, S. Yamaguchi, S. Irle, K. Itami, *Org. Biomol. Chem.* **2012**, *10*, 5979–5984.

[31] E. Kayahara, T. Kouyama, T. Kato, H. Takaya, N. Yasuda, S. Yamago, *Angew. Chemie - Int. Ed.* **2013**, *52*, 13722–13726.

[32] N. Toriumi, A. Muranaka, E. Kayahara, S. Yamago, M. Uchiyama, *J. Am. Chem. Soc.* **2015**, *137*, 82–85.

[33] E. Kayahara, T. Kouyama, T. Kato, S. Yamago, *J. Am. Chem. Soc.* **2016**, *138*, 338–344.

[34] Y. Masumoto, N. Toriumi, A. Muranaka, E. Kayahara, S. Yamago, M. Uchiyama, *J. Phys. Chem. A* **2018**, *122*, 5162–5167.

[35] The association constant (K_a) was estimated on the basis of chemical shift of the aryl proton by using a curve fitting program. S. Akine, *TitrationFit, Ver 1.1.3, for Analysis of Titration Data in Host-Guest Chemistry,* **2013**.

[36] E. G. Hohenstein, C. D. Sherrill, *Wiley Interdiscip. Rev. Comput. Mol. Sci.* **2012**, *2*, 304–326.

[37] R. M. Parrish, L. A. Burns, D. G. A. Smith, A. C. Simmonett, A. E. DePrince, E. G. Hohenstein, U. Bozkaya, A. Y. Sokolov, R. Di Remigio, R. M. Richard, J. F.

Gonthier, A. M. James, H. R. McAlexander, A. Kumar, M. Saitow, X. Wang, B. P. Pritchard, P. Verma, H. F. Schaefer, K. Patkowski, R. A. King, E. F. Valeev, F. A. Evangelista, J. M. Turney, T. D. Crawford, C. D. Sherrill, *J. Chem. Theory Comput.* **2017**, *13*, 3185–3197.

[38] The return reaction, regeneration of the inclusion complex (**2**), was partially proceeded by treating the mixture of dication ($\mathbf{2}^{2+}$) and **G1** with Zn powder (see supporting information Figure S26)

[39] (a) J. F. Stoddart, *Angew. Chemie - Int. Ed.* **2017**, *56*, 11094–11125. (b)

[40] S. Fa, T. Kakuta, T. Yamagishi, T. Ogoshi, *Chem. Lett.* **2019**, *48*, 1278– 1287.

[41] Y. Xu, R. Kaur, B. Wang, M. B. Minameyer, S. Gsänger, B. Meyer, T. Drewello, D. M. Guldi, M. Von Delius, *J. Am. Chem. Soc.* **2018**, *140*, 13413–13420.

[42] M. Yokoya, S. Kimuira, M. Yamanaka, *Chem. Eur. J.* **2021**, *27*, 5601–5614.